Chapter 3

THE VITREOUS HUMOR: MECHANICS AND STRUCTURE

3.1 Primary Structure and Composition

As described in Chapter 1, the vitreous humor is a delicate, transparent gel composed of a highly-hydrated double network of protein fibrils and charged polysaccharide chains (Figure 1). By weight, vitreous is ~ 99% water and 0.9% salts.[1] The remaining 0.1% is divided between protein and polysaccharide components. Most of the protein is found in or associated with 10-20 nm heterotypic collagen fibrils composed of a small collagen type V/XI core wrapped in a thick layer of collagen type II (75% of the fibril by mass). The exterior of each fibril is decorated with covalently-bound collagen type IX and other glycoproteins. Collagen IX contains four short, coiled noncollagenous domains separated by three triple-helical collagenous domains. Two of the collagenous domains are aligned with, and crosslinked to, the axis of the fibrils, but the third strut-like collagenous domain is sterically forced to project out from the fibril by a heparin-sulfate glycosaminoglycan (GAG) chain that is covalently bound to the adjacent, hinge-like noncollagenous domain.[1]
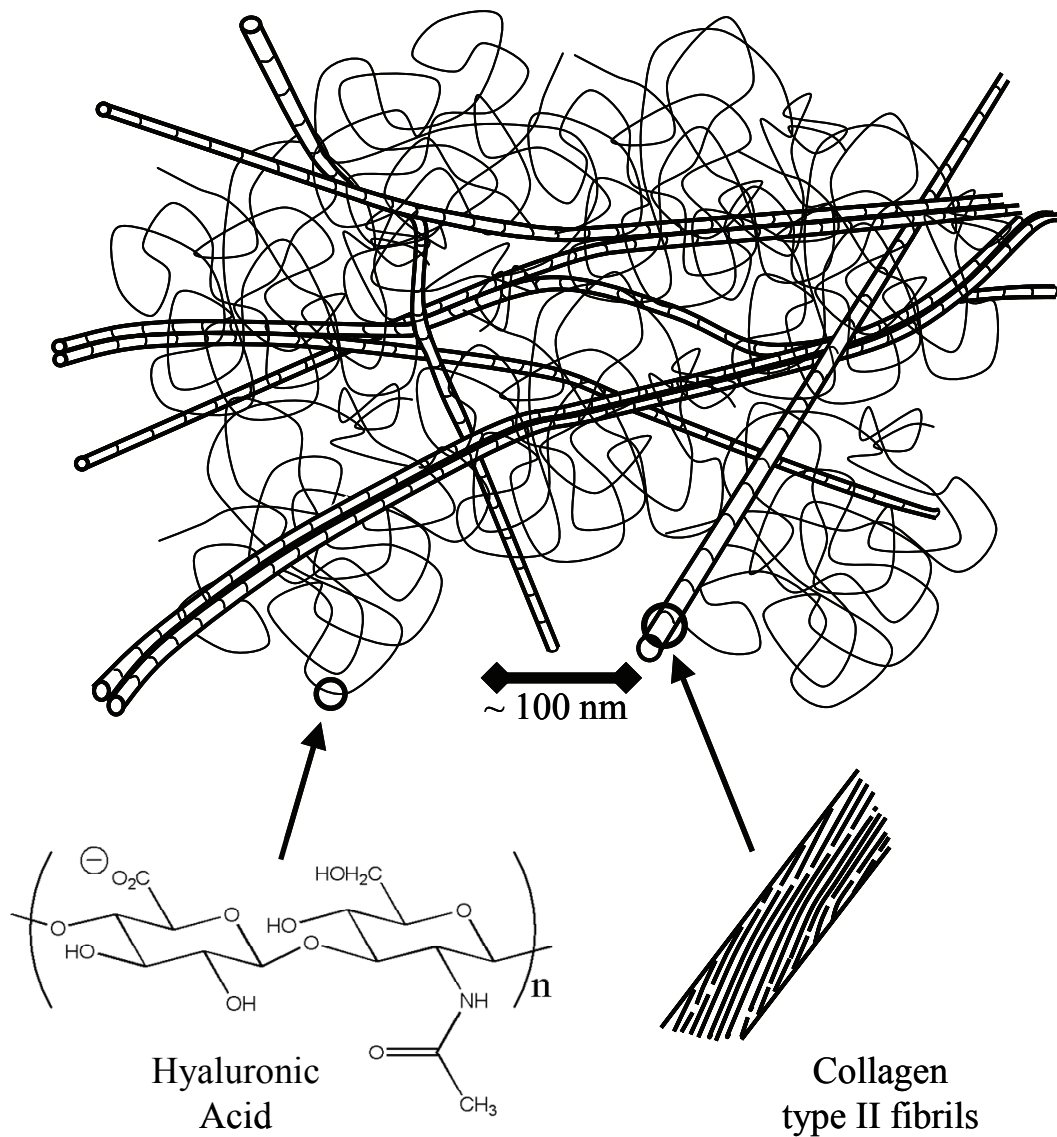
Figure 1. Schematic depiction of the network structure of the vitreous. The vitreous is composed of a highly-swollen double network of collagen type II fibrils (~ 15 nm in diameter) and hyaluronic acid (~ 5M MW).

Most of the collagen fibrils originate in the vitreous base – a band of peripheral vitreous that stretches from just behind the plane of the lens and zonules back to the meridian of the eye. The high concentration of protein fibrils in the vitreous base drops as the collagen fibrils fan out and fill the vitreous cavity. After the fibrils diverge they approach the retina

at various points around the periphery and insert into the inner limiting membrane where they turn and run in the posterior direction to the optic nerve, following the curvature of the eye.[2] Collagen fibrils are hydrophobic and adhere to each other when they come in contact; thus, the fibrils of the vitreous continuously merge with and diverge from lateral aggregates as they traverse the length of the eye.[3] A sufficient number of fibrils are also oriented nasal-temporally to form a fully crosslinked network.

While extensive progress has been made in identifying the components and biochemistry of the vitreous, lack of sufficient experimental methods has hampered previous efforts to quantitatively define its mechanical properties and nano-scale architecture. The lubricating ability of its constituent molecules and its fragile network structure have made reliable measurements extremely difficult. A number of creative methods have been devised to measure the gel character of the vitreous, including bulk measurements,[4-6] magnetic microrheology,[7-9] *in vivo* visual tracking for humans,[10] and more recently, acoustic techniques.[11] These techniques allow for comparative analyses, but cannot give insight into the molecular mechanisms responsible for the observed bulk behavior. A few of these authors estimate the moduli of the vitreous, but the present results suggest that these values are systematically low for bovine and porcine vitreous— in some cases by orders of magnitude.

The network of collagen fibrils has been presumed responsible for the mechanical properties of the vitreous because of the load-bearing capacity of collagen and because the vitreous does not fully collapse with enzymatic removal of hyaluronan.[1, 2, 12] It has been suggested that swollen hyaluronan (HA) polysaccharide chains play a passive role in the

vitreous by filling the space between the fibrils to prevent extensive aggregation. Prior literature indicates that the vitreous shrinks after removal of hyaluronan[1-3], and morphologically the collagen network "relaxes" from having relatively straight to significantly curved fibrils.[3]

These "relaxation" and shrinking observations appear to be more significant than previously thought: they are manifestations of an additional, structural role for hyaluronan. We present rheological and biochemical evidence that hyaluronan contributes significantly to the *elastic* character of the vitreous *in vivo*. Specifically, hyaluronan swells, stretching the network of rope-like collagen fibrils to a state of tension and increasing the rigidity of the network (Figure 2). When removed from the confines of the retina, HA is rapidly driven out of the vitreous to release the network tension. We present evidence that the shrinking that occurs after dissection is due to the loss of HA.
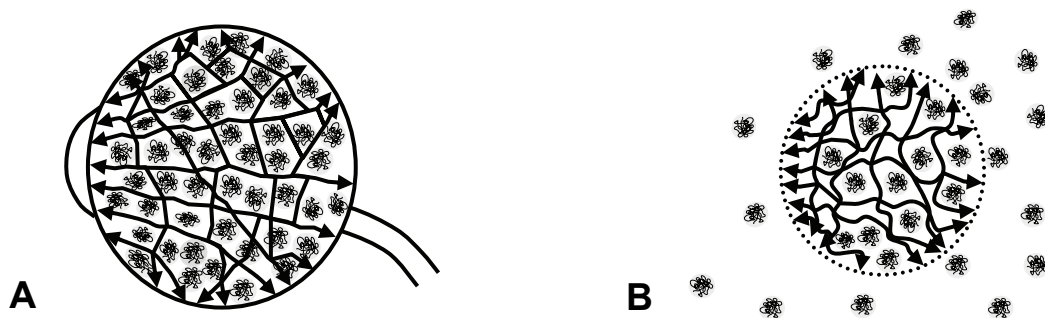

Figure 2. Schematic depiction of the collagen fibrils (heavy lines) of the vitreous network under tension and after relaxation. (A) Native state of the vitreous in the eye and (B) after relaxation by release of hyaluronan (thin coils) after removal from the eye.

To address wall-slip and accommodate the fragile vitreous tissue, two significant experimental challenges imposed by the structure of the network, we have employed the cleat geometry[13] for dynamic shear rheometry (Chapter 2). This tool has allowed us to quantitatively measure the shear moduli of the vitreous directly using a fluids rheometer. The cleat geometry suppresses wall slip while causing minimal disturbance to tissue structure (see Chapter 2). We have also used this tool to track the softening that occurs after the vitreous is extracted from the eye. These results, in conjunction with observations that HA is actively forced out of the vitreous after removal from the eye, suggest a modified view of the network structure of the vitreous in which internal tension from the swelling of HA significantly increases the stiffness of the tissue *in vivo*. Overcoming the obstacles to measuring the shear moduli of the vitreous is also an essential step forward in defining target mechanical properties for potential vitreous replacement materials and evaluating pharmacological vitrectomy agents. In addition to quantitative results for bovine and porcine vitreous, qualitative results for human vitreous are presented.

3.2 Materials and Methods

Fresh porcine eyes (< 36 hours *post mortem*, stored at 5° C in physiological saline prior to arrival) were acquired through Sierra for Medical Science (Santa Fe Springs, CA). All pigs were 3 – 6 month old Chester Whites, weighing 50 – 100 kg and in good health at the time of slaughter. Human donor eyes were obtained through the National Disease Research Interchange (a service of the NIH, Philadelphia, PA). Permission was obtained specifically for research use of the human eyes; they were unsuitable for cornea transplants. Approval

was also obtained from the Caltech Internal Review Board (Appendix A). Eyes were gently dissected to remove the vitreous with minimal disruption. All human specimens were tested between 28 and 48 hours *post mortem*; storage as an intact globe for up to 60 hours *post mortem* did not affect rheological results as previously observed.[14] Intact vitreous was either used directly or a disc-like section was cut with the axis of the disc coinciding with the anterior-to-posterior axis of the eye (typically 1.5 – 2.5 g). Some of the vitreous discs were loaded into a cleated 25 mm parallel disc geometry for mechanical characterization, and the remainder were used for network stability studies. Cone-and-plate geometries are inappropriate for chemically crosslinked gels because high compression near the center of the tool induces a non-uniform normal force profile and destroys the vitreous network.

Mechanical measurements were made on an ARES-RFS fluids rheometer from TA Instruments, Inc. (New Castle, DE) using our novel cleat geometry to overcome slip.[13] Previously reported methods for overcoming wall slip such as roughened plates or sandpaper were insufficient because the upper boundary of the vitreous develops a lubricating layer. Cleated tools succeed by penetrating the lubricating boundary layer to achieve an effective no-slip boundary condition (Chapter 2). All measurements were made in a closed, humid atmosphere at 20° C and with zero normal force on the samples. Shear moduli were monitored as samples were subjected to oscillatory strain ($\gamma = 3\%$) at a fixed frequency ($\omega = 10$ rad/s) for up to 90 minutes Longer experimental times were precluded by drying of the sample edges, which artificially raised the apparent modulus of the samples. The conditions for these experiments were chosen based on the results of variable

frequency (γ = 3%, ω = 1 - 50 rad/s) and variable strain (ω = 10 rad/s, γ = 0.5 – 100%) experiments. The initial modulus values are very sensitive to the length of time that elapses between dissection and rheological testing. Therefore, dissection time was kept as uniform as possible (2 – 3 minutes) and tissue was transferred to the instrument immediately after dissection was completed.

In addition to oscillatory tests, steady (shear) rate tests were conducted to determine the minimum shear stress and strain required to destroy the tissue. These "failure" tests were conducted after loading vitreous specimens and watching the moduli reach steady state in oscillatory shear (Figure 3). Then a steady shear rate ($\dot{\gamma}$ = 0.1 s^{-1}) was applied for 150 seconds while continuously monitoring the resulting shear stress. Higher and lower shear rates ($\dot{\gamma}$ = 0.3 and 0.01 s^{-1}) were also probed separately to demonstrate the rate dependence of the transient shear stress.

The discovery that vitreous loses elasticity and exudes fluid after dissection motivated us to measure the time-dependent mass loss and the composition of the exuded fluid. Post-dissection mass loss was measured in four different environments denoted A-D: (A) an intact vitreous body was placed in a dry Petri dish and covered; (B-D) central discs of vitreous were placed in covered Petri dishes that were either (B) dry, (C) filled with isotonic saline, or (D) filled with mechanically liquefied vitreous from other eyes. Liquefied vitreous was obtained by removing the vitreous of three to six fresh eyes of the same species immediately prior to the experiment and slicing them into small fragments, which caused much of the vitreous to liquefy. The mass of each vitreous sample was measured immediately after removal from the eye (Mass$_o$) and only once at the end of the

treatment period, which ranged from 5 to 120 minutes ($Mass_f$) – excess handling damages the vitreous and artificially accelerates weight loss. The treatment periods ranged from 5 to 120 minutes. One specimen was subjected to condition A and photographed at 1, 10, 30, and 90 minutes from the moment it was placed in the Petri dish. Using condition C, the components exuded into the saline solution were analyzed for hyaluronic acid (Hyaluronic Acid Test Kit; Corgenix, Inc., Denver, CO) and the presence of protein (ninhydrin assay). The circular dichroism spectrum of the bath solution of condition C was measured after 120 minutes and compared with spectra from solutions of purified collagen type II and hyaluronic acid obtained at room temperature with a model 62DS Circular Dichroism Spectrometer, AVIV Associates (Lakewood, NJ).

3.3 Mechanics of the Vitreous – the Key to Structure

In accord with prior literature, it appears that the connectivity of the gel network, while not completely homogeneous, is well distributed throughout most of the tissue.[1, 15] One consequence of this structural homogeneity is that central vitreous collapses at the same rate as intact, whole vitreous (i.e., removal of the peripheral tissue does not accelerate the shrinking rate). A second consequence is that the mechanical stability of a central disk of vitreous reflects the properties of the whole – a key assumption in our rheological experiments.

The dynamic moduli of vitreous sections decay monotonically to a significantly lower, steady-state value that persists thereafter (Figure 3). The average initial storage and loss moduli of bovine vitreous were $G'_{init} = 32 \pm 12$ Pa (mean $\pm$ SD) and $G''_{init} = 17 \pm 7.0$ Pa

(n=17); and for porcine vitreous $G'_{init} = 10 \pm 1.9$ Pa and $G''_{init} = 3.9 \pm 0.8$ Pa (n=9). The

large standard deviations reflect rapid initial changes, making the observed moduli

sensitive to the precise time from dissection to loading. Smaller standard deviations for

porcine samples were achieved by using a consistent loading time of approximately 1

minute from removal of the dissected globe to inception of measurement. The average

steady-state moduli for bovine vitreous were $G'_{fin} = 7.0 \pm 2.0$ Pa and $G''_{fin} = 2.2 \pm 0.6$ Pa;

and for porcine vitreous $G'_{fin} = 2.8 \pm 0.9$ Pa and $G''_{fin} = 0.7 \pm 0.4$ Pa.
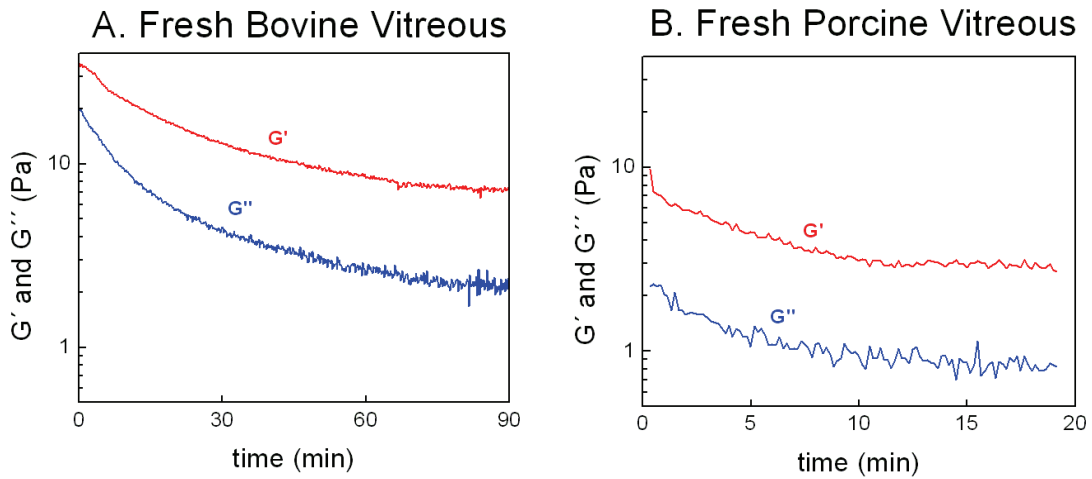

Figure 3. Typical time sweep of fresh bovine (A) and porcine (B) vitreous samples showing the rapid modulus decay to a steady-state after removal from the eye ($\gamma = 3\%$, $\omega = 10$ rad/s). The loss tangent reached steady-state more rapidly, often in as little as 20 minutes in bovine (tan $\delta = 0.31 \pm 0.03$) and 2 minutes in porcine (tan $\delta = 0.24 \pm 0.09$) specimens.

The drastic drop in shear modulus indicates a significant molecular-level change from a

relatively rigid *in-oculo* state, which is not stable outside of the constraints of the eye, to a

measurably softer state *ex-oculo*. Therefore, the initial moduli may be closer to the moduli

of the vitreous *in vivo* and the steady-state moduli represent a lower bound on the *in vivo* moduli, perhaps as much as five times lower. Nevertheless, these steady-state moduli are significantly *greater* than previously reported values,[4, 6, 9, 10] by orders of magnitude in some cases (Figure 4). Additionally, time-dependent modulus changes have not previously been reported. An interpretation of the time-dependent modulus changes as well as structural differences between the initial and steady states will be examined in the next section.
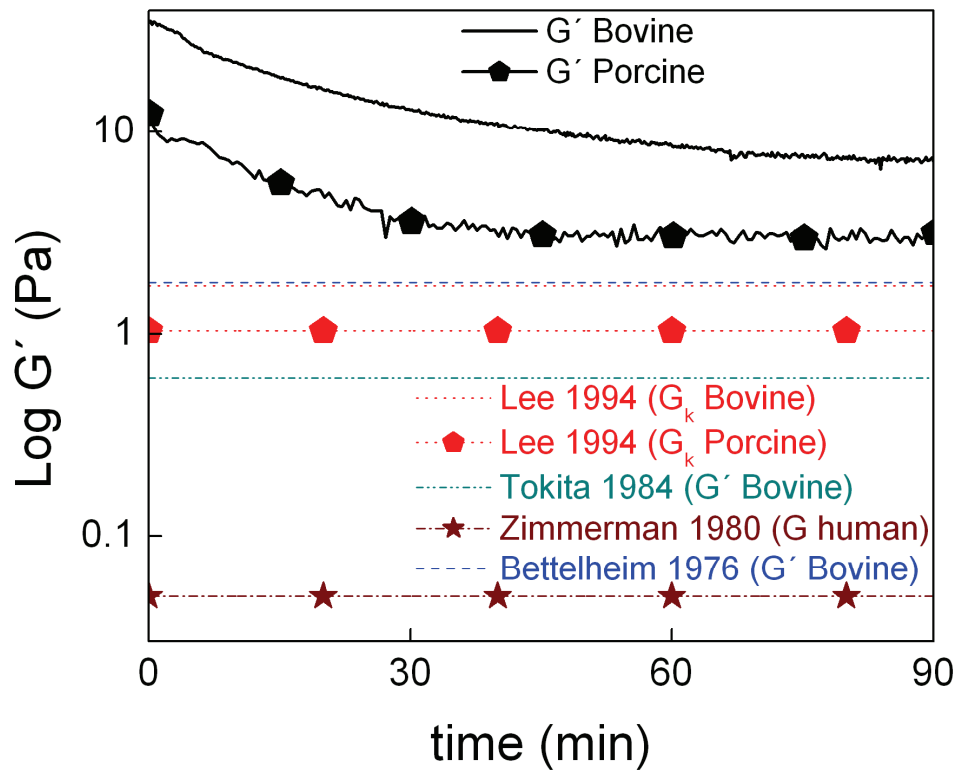

Figure 4. Typical time-dependent behavior of G' at fixed strain amplitude (3%) and frequency (10 rad/s) for bovine and porcine vitreous. Estimates of the modulus based on prior literature are indicated for reference.

The strain amplitude (3%) and frequency (10 rad/s) for vitreous analysis were optimized

to allow us to apply gentle deformations close to the linear regime of the gel network.

Variable strain experiments conducted at 10 rad/s show that the porcine vitreous is linear

just below 3% strain and weakly non-linear thereafter (Figure 5). The "linear" or "strain-

independent" regime indicates that the level of strain applied is small enough not to perturb

the structure of the material. In biological specimens, the mechanical properties of the

linear regime are particularly interesting because it includes normal physiological loads.

Thus, linear viscoelastic properties represent the normal response of many tissues *in vivo*.

In order to optimize the signal-to-noise ratio for these soft samples, oscillatory shear

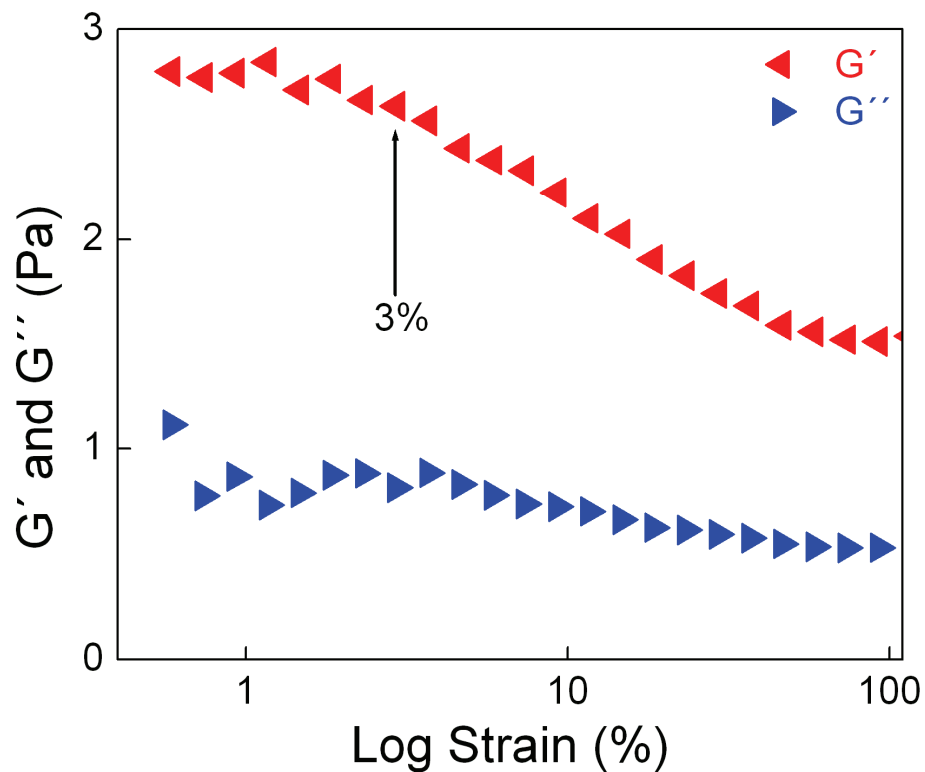experiments were conducted near the upper limit of the linear regime at 3% strain.

Figure 5. Typical variable strain experiment conducted after the
shear modulus of the vitreous had reached steady-state (Porcine

vitreous ~ 20 minutes after loading, frequency=10 rad/s). 3%
strain is just above the linear regime but lower strains do not
generate sufficient torque for accurate determination of moduli.

Regarding the frequency dependence of the dynamic moduli: the storage modulus of

steady-state porcine vitreous varies weakly with frequency up to ~ 5 rad/s and rises

significantly thereafter (Figure 6). This frequency dependence is typical of a lightly cross-

linked amorphous network of macromolecules[16] – consistent with the accepted model of

vitreous structure. The broad plateau modulus region expected for gels appears below ~ 5

rad/s. To generate sufficiently large torques for the instrument specifications while

operating at small strain amplitudes, a frequency of 10 rad/s was required. Thus, the moduli

we report may be somewhat higher than the gel's steady-state plateau modulus. The strain

and frequency dependencies of bovine vitreous are similar to the porcine data shown.
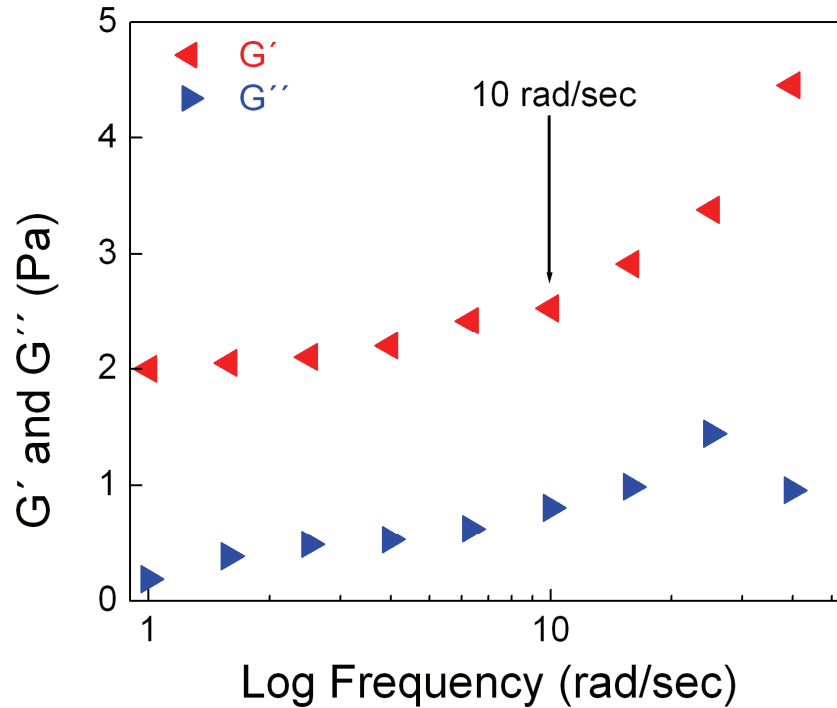
Figure 6. Typical variable frequency experiment conducted after the shear modulus of the vitreous had reached steady-state (porcine vitreous, $\gamma = 3\%$). 10 rad/s is slightly above the plateau regime, but lower frequencies do not generate sufficient signal for accurate modulus measurements at low strain amplitude.

A limited number of matched pairs of human donor eyes were analyzed using the protocols developed above for porcine and bovine eyes (Figure 7). The mechanical properties of human vitreous appear to be highly variable between individuals. With one exception, however, fellow eyes had very similar properties. This, taken together with the large difference between the two 21 year old donors, suggests that the large standard deviation seen in porcine eyes comes as a result of sample-sample variability and not inconsistencies in the measurement method.
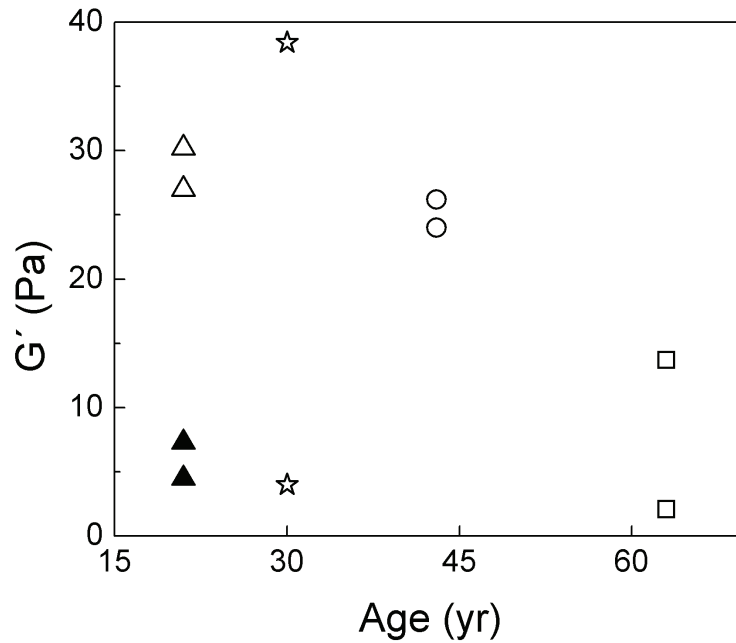
Figure 7. Initial shear moduli of matched human donor vitreous as a function of donor age. Experimental parameters developed for bovine and porcine eyes were used (γ = 3%, ω = 10 rad/s). Matching symbols denotes matched pairs.

In addition to linear viscoelastic properties, tissue failure under high stress is relevant to certain injuries and surgical procedures. During severe head trauma, the vitreous gel can be torn and cause retinal tears. Also, during vitrectomy procedures performed to treat diabetic retinopathy, among other major eye diseases, surgeons need to destroy the vitreous in order to remove it from the eye. However, to our knowledge, there have been no published studies that demonstrate the maximum stress load the vitreous can bear, nor have studies demonstrated the response of the tissue when stress exceeds this maximum and the tissue fails. We have addressed this need using steady-shear experiments in which the vitreous specimens are sheared (at a constant rate) to the point of failure.

The failure patterns of the vitreous demonstrate a natural protective effect against head trauma and provide new considerations for vitreous surgery. Shear stress rises sharply at the onset of strain, rapidly reaches a rate-dependent maximum (failure stress and strain increase with shear rate), and then gradually declines (Figure 8). Thus, the vitreous is relatively soft when deformed slowly; however, it stiffens considerably against rapid deformations—possibly a protective mechanism for the retina during head trauma. In the context of vitreous surgery, this failure pattern suggests that removing the vitreous quickly puts unnecessary stress on the retina. The need for slow vitreous removal appears even more important in light of the gradual decline in stress that occurs even after failure; the vitreous can continue to transfer stress to the retina even after it has failed.
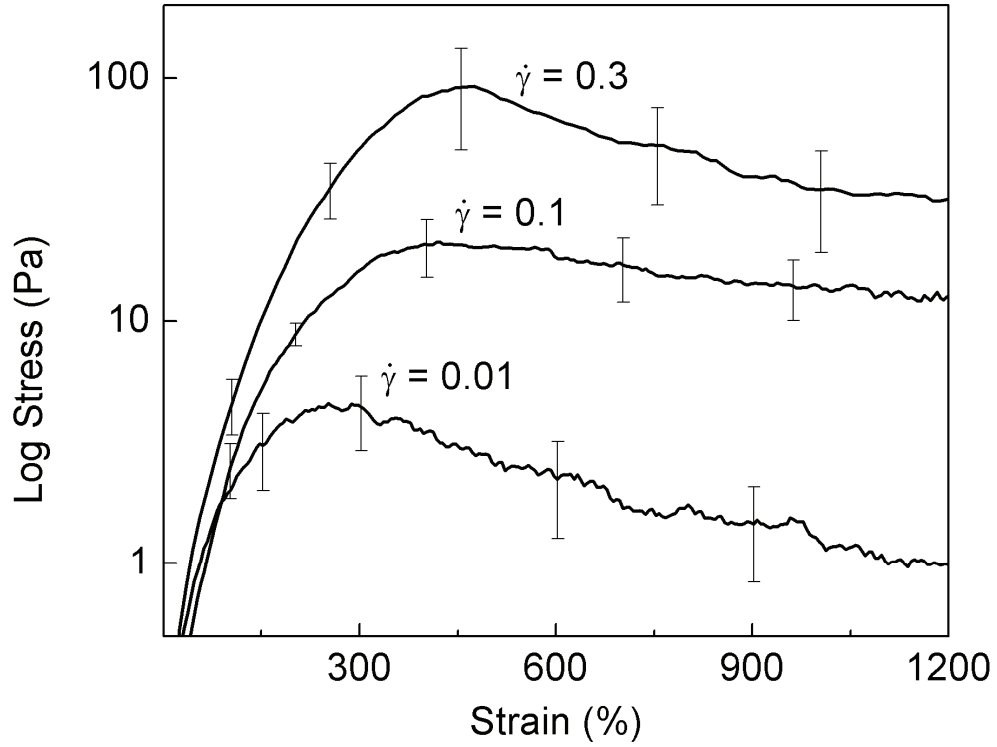
Figure 8. Average failure behavior of porcine vitreous strained under steady shear at three different shear rates (0.01, 0.1, and 0.3 s^{-1}; n ≥ 3).

Shearing at lower rates appears to allow the network to relax, thereby reducing the stress at any given strain. Based on the frequency dependence of the storage modulus in oscillatory tests, a shear rate of $\dot{\gamma}$ = 0.1 s^{-1} is sufficiently slow to allow the high frequency relaxation processes evident at ω > 5 rad/s to relax. However, slower relaxation mechanisms are apparently active under high strains because a lower shear rate ($\dot{\gamma}$ = 0.01 s^{-1}) decreases the failure stress from σ_{max} = 24 ± 3 Pa ($\dot{\gamma}$ = 0.1 s^{-1}) to σ_{max} = 5.7 ± 0.9 Pa ($\dot{\gamma}$ = 0.01 s^{-1}) and failure strain from γ_{fail} = 418 ± 51 Pa ($\dot{\gamma}$ = 0.1 s^{-1}) to γ_{fail} = 259 ± 35 Pa ($\dot{\gamma}$ = 0.01 s^{-1}). The distribution of relaxation times and gradual failure also indicate significant heterogeneity in

the network; short, thin collagen fibrils break under small strains, while larger and longer filaments last longer, breaking only after large deformations (beyond the peak stress).

3.4 Mass Loss Associated with Post-Dissection Softening

Upon removal of the test samples from the rheometer, two obvious changes in the tissue confirm that the steady-state moduli are lower than the moduli of the vitreous *in vivo*. First, the post-rheology vitreous appears to sag, elongating far more when lifted with forceps. The reason for the softening may be found in the second major observation: a small puddle of liquid is left behind on the instrument where aqueous material has seeped out of the vitreous.

To explore the possible connection between the loss of aqueous material and rheological changes in freshly extracted vitreous, we observed changes in mechanical integrity and mass as a function of time (Figure 9). Immediately following dissection, the vitreous partially retains the native shape of the vitreous cavity. After being placed in a sealed Petri dish for 10 minutes, the vitreous has visibly lost fluid and elongates upon lifting. This trend continues until 90 minutes after dissection, when the specimen reaches its post-dissection steady state. Morphological changes coincide with mass loss, which was rapid immediately after removal from the eye but stabilized within 2 hours.

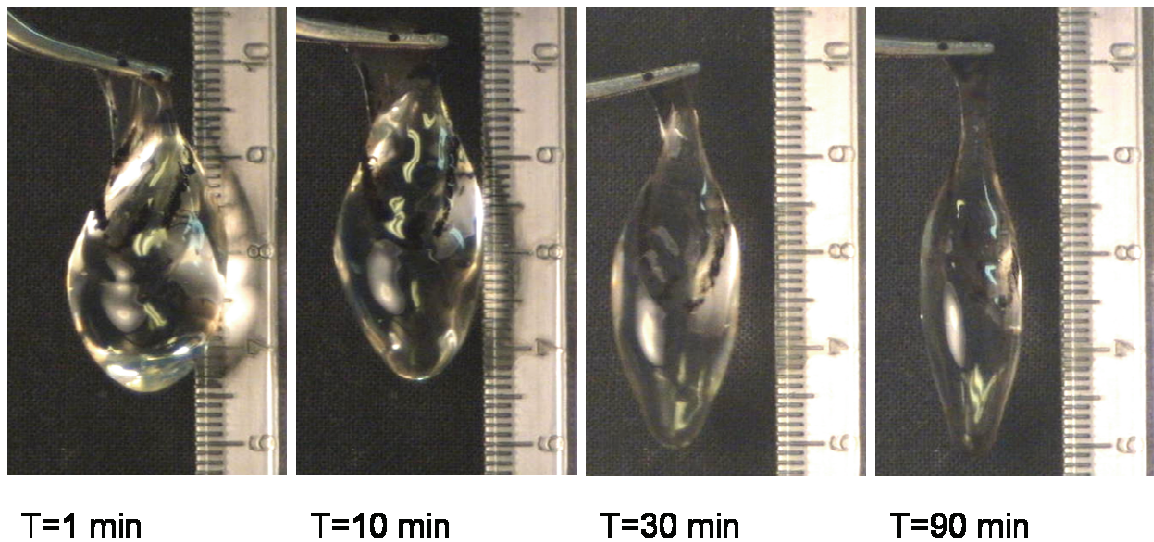T=1 min   T=10 min   T=30 min   T=90 min

Figure 9. This sequence of photographs illustrates the state of a whole vitreous gently removed from a fresh porcine eye 1, 10, 30, and 90 minutes after dissection. The vitreous was kept in a dry, covered Petri dish during the course of the experiment.

The ejected fluid was rich in hyaluronan and soluble protein (presumably albumin), but contained no detectable helical collagen. In condition C, more than 10% of the vitreous HA was ejected after 120 minute, as determined by enzyme-linked hyaluronic acid binding protein assay. The loss of protein was not as great; $\leq 10\%$ of the total protein was ejected, as measured by the ninhydrin amino acid assay. The circular dichroism spectrum of the ejected fluid is characteristic of albumin, but not collagen (Figure 10). Because slightly more than 10% of the total vitreous mass (volume) was also lost, it appears that the ejected fluid contained the soluble components of the vitreous in roughly the same proportions as the vitreous itself. Fluid loss was very similar in bovine and porcine vitreous.
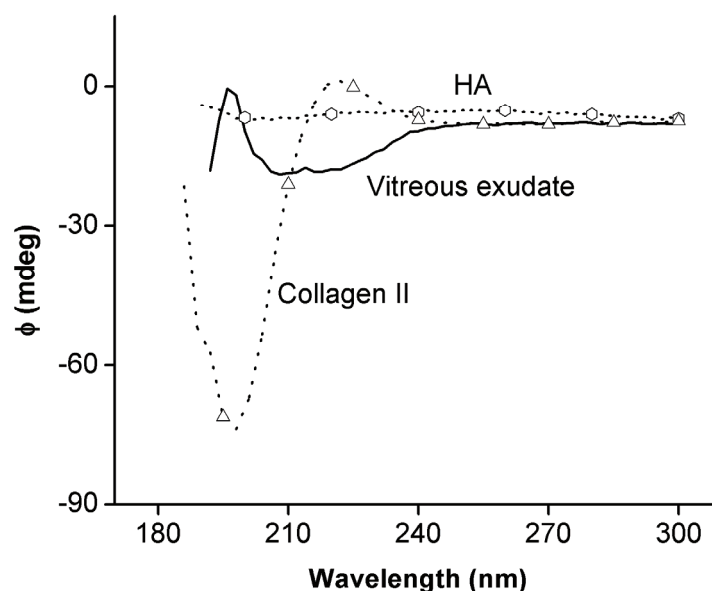
Figure 10. Circular dichroism spectrum of conition C exudate compared with spectra of collagen type II and HA standards at room temperature.

To quantify the liquid-loss observations, we extracted fresh vitreous specimens and placed them under the four conditions listed in the methods section (A—Whole vitreous placed in covered Petri dish, B, C, and D—Disc shaped vitreous sample placed in covered Petri dish either dry [B], filled with isotonic saline [C], or filled with liquefied vitreous [D]). The mass-decay period started immediately after the vitreous body was removed from the eye. Regardless of the conditions under which the vitreous was placed, the mass dropped 5 to 10% within the first 5 minutes. Thereafter the mass of A and B dropped monotonically, with A continuing to drop below 50% of its initial mass and B reaching a near-equilibrium value near 75% within 1 hour (Figure 11). The masses of C and D dropped only slightly between 10 and 120 min. to ~90% of their initial mass. The masses of A and B continued to drop monotonically after 10 min., and fluid continued to seep out of the vitreous body.
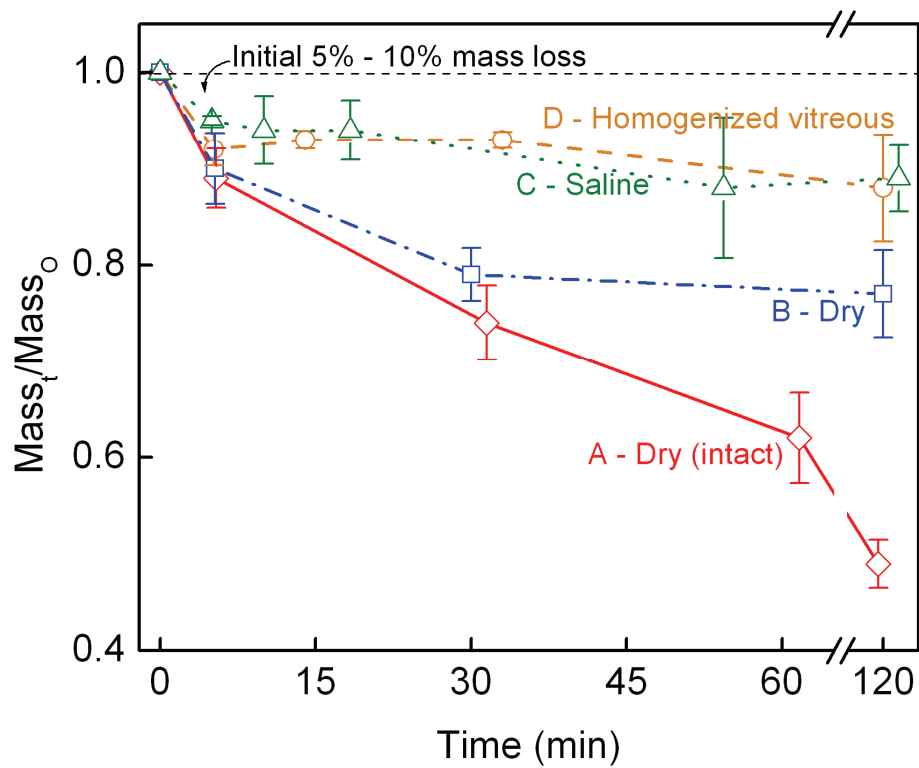
Figure 11. Changes in porcine vitreous sample weight monitored over time under the following conditions: whole vitreous placed in covered Petri dish (A), central section of vitreous placed in covered Petri dish that is dry (B), contains isotonic saline (C), contains mechanically liquefied vitreous (D) (n = 4).

The differing magnitudes of mass loss under conditions A – D provide insight into the mechanisms that drive mass loss. In A there is a significant and continuing driving force for expulsion of fluid. Two obvious driving forces are gravity (the globe collapsing under its own weight) and wetting/diffusion (fluid diffuses out of the tissue along the concentration gradient). The same diffusion forces are present in both A and B, however, the disk shape of B has less gravitational potential energy. Because all other factors are equal, B appears

to retain a greater fraction of its mass due to the smaller gravitational driving force for fluid loss. It was surprising that cutting sample B did not increase the mass loss as compared with A but actually had the opposite effect.

Conditions C and D are significantly different from A and B because the two obvious fluid-loss driving forces (gravitational collapse and concentration gradient-driven diffusion) have been eliminated. In C, the saline bath allows the vitreous to float at neutral buoyancy in a solution that is isotonic with the primary soluble component of the vitreous – NaCl. In D, the vitreous is completely surrounded by other vitreous material – thereby completely eliminating the concentration gradient for all components, including hyaluronic acid. Despite these changes there is still a mass loss on the order of 7% in the first 5 – 10 minutes. This rapid initial weight loss appears to be driven by an internal force that becomes imbalanced when the *in-vivo* constraints on the vitreous are removed. It is also coincident with the sharp initial drop in shear modulus (Figure 2). We will present a novel hypothesis that links these two phenomena and suggest two possible underlying mechanisms.

3.5 Network Tension – the Contribution of Hyaluronic Acid

The loss of hyaluronan-rich fluid from the vitreous was unexpected and provides several clues to the mechanism driving fluid loss and modulus drop. The observations regarding potential mechanisms of fluid loss reported in Section 3.4, that a significant portion of the fluid loss is neither driven by diffusion down a gradient nor by gravity, and that the rate and magnitude of fluid loss are independent of sample surface area, combine to suggest that

hyaluronan is not simply diffusing out of the vitreous but, rather, that it is driven out. Furthermore, the driving force must be present throughout the volume of the vitreous. Based upon these observations and the correlation between fluid loss and modulus decrease, we suggest that the driving force for this fluid expulsion is tension in the collagen network induced by hyaluronan.

It is well accepted that hyaluronan draws water into the fibril network to achieve Donnan equilibrium, adds chemical stability to the collagen, and separates the fibrils.[1, 3, 12] Polyelectrolytes such as HA are swollen by the hydration spheres of their associated counter ions.[17] Counter ions also increase the entropic cost of overlap because a single overlap event between two polymers results in the doubling of the local concentration of many counter ions. The expanded configuration of HA, combined with its resistance to overlap, make it ideal for accomplishing the functions listed above. The literature, however, makes no firm assertions concerning contributions of hyaluronan to the elasticity of the gel.[1, 3, 12] Using the cleat geometry we have been able to monitor the evolution of the moduli after dissection and, thereby, gain new clues that suggest that hyaluronan does stiffen the gel. We propose that hyaluronan increases the moduli of the vitreous by placing the collagen network under internal tension as it swells to find a Donnan equilibrium hydration state (Figure 1A vs. 1B). Tension on individual collagen fibrils would reduce their ability to deform and, thereby, increase the modulus. If the vitreous is approximated as a contracting, isotropic sphere, the average measured mass reduction in C and D in the first 5 minutes (7%) corresponds to a 7% volume contraction and ~ 2% radial contraction.

Two possible mechanisms by which hyaluronan could induce network tension through a small stretch (~ 2%) are consistent with the fact that hyaluronan is essentially retained in the vitreous. The vitreous is enveloped in a semipermeable membrane. One possible source of network tension is the hydrostatic pressure (due to hyaluronan-induced Donnan swelling), which exerts an outward force on the semipermeable periphery of the vitreous network until the collagen fibrils are pulled taut. Semiflexible polymers exert an entropically driven elastic force when their end-to-end distance is increased beyond its equilibrium value.[18] Thus, in a taut state, fibrils are loosely analogous to long elastic ropes that are stretched by the swollen HA. Upon release of the boundary constraints, the HA is driven out of the network as the stretched ropes contract to a tension-free length. However, physical entanglements due to the high molecular weight (~ 5 million) of HA prevent it from exiting immediately. There is also evidence to suggest that HA is anchored to the collagen network and not just physically entangled, which would further slow the loss of HA.[19] There is a modest HA concentration gradient in the vitreous, with the highest concentration located in the posterior of the eye.[2] If HA were completely free to diffuse through the vitreous, even if motion were slowed by entanglements one would anticipate that HA would distribute itself homogeneously throughout the eye eventually.

A second possible tension mechanism arises if the hyaluronan is indeed bound to the network strands, be it directly or through binding mediators. As explained previously, each hyaluronan molecule must retain its hydration volume. If the HA molecules are bound to fibrils, crowding between two neighboring hydration spheres would effectively drive the attachment points of the two HA molecules to separate. The fibril would extend either

until the chemical potential of swelling was balanced by the fibril's conformational entropic loss or to the limit of full extension. Just as in the first case, HA swelling would induce internal tension that would be distributed throughout the collagen network. These two mechanisms are not mutually exclusive, so both may contribute. And in both cases, removal from the eye would provide a thermodynamic driving force for an efflux of hyaluronan-rich fluid.

Both scenarios are similar and consistent with all of our observations. In both cases, any portion of the network should behave the same as the intact vitreous. The accuracy of this "homogeneous properties" prediction can be verified by comparing the weight-loss behavior of conditions A and B of the previous section. Biochemical assays also demonstrated that the ejected fluid was rich in HA. In both cases, loss of fluid should cause the vitreous to soften even though the concentration of collagen in the shrunken network is higher than in the swollen state. Both internal tension mechanisms are also in accord with Bos's microscopic observation that the collagen network appears to "relax" after the removal of hyaluronan.[3]

To envision the feasibility of crowding of hyaluronan in the vitreous – a key feature of both models – we calculated the maximum volume available to each hyaluronan molecule and compared it with the volume that an isolated hyaluronan polymer of the same molecular weight would occupy under physiological conditions. We calculated the volume available per hyaluronan molecule in the vitreous using literature hyaluronan concentration and molecular weight values to evaluate the following expression:[1]

$$Volume = \cfrac{1}{\left[HA\ concentration\left(\mu g \middle/ ml \right) \right] \times \left(1 \middle/ molecular\ weight \right) \times N_A}$$

We estimated the volume that a hyaluronan molecule of the species-appropriate molecular weight occupies at 37° C and 150 mM NaCl based upon radius-of-gyration (R_g) values given by Mendichi.[20] These calculations were performed for human ([HA] = 65 – 400 μg / ml, MW = 3.5 x 10^6 g / mol, R_g = 260 nm) and bovine ([HA] = 560 μg / ml, MW = 2.36 x 10^5 g / mol, R_g = 90 nm) vitreous. The bovine molecular weight value was chosen from within the range listed[1] because of available R_g data.[20] Based upon $\frac{4}{3} \times \pi \times R_g^3$, in humans a typical molecule of vitreous hyaluronan would occupy 7.4 x 10^{-14} ml, fully filling the 1.4 x 10^{-14} to 8.9 x 10^{-14} ml space available. In the bovine case, one vitreous hyaluronan molecule would occupy 7.0 x 10^{-16} ml, while 6.9 x 10^{-16} ml per hyaluronan molecule is available *in vivo*. The values are approximate since hyaluronan is not evenly distributed through the vitreous. However, the close match between average space available in the vitreous and average single chain volume suggests that there are not large void volumes between hyaluronan molecules *in vivo*.

While this is the first evidence that network tension stiffens the vitreous, the concept of hydrostatic structures, or "hydrostats," is well accepted in the biomechanics literature.[21] One notable example of hydrostatic pressure contributing to mechanical strength is cartilage.[21, 22] Like the vitreous, cartilage consists of a hydrated network of collagen II fibrils filled with highly-charged HA. Cartilage has a much higher modulus due to its higher protein content, but the underlying mechanism is the same – Donnan swelling due to

the high fixed charge density stiffens the tissue by extending the collagen fibrils of the network.

Our internal tension model suggests that the initial value of the modulus, measured within minutes of dissection, may resemble the mechanical properties of tissue *in vivo*, where the collagen fibrils are stretched. Steady-state moduli represent essentially the same collagen network, with the same degree of connectivity but with a reduced presence of HA and no net tension. While it appears that our steady-state moduli are systematically lower than *in vivo*, they are also useful for several reasons. First, while they represent minimum values for the native moduli, they are higher than any previous estimates found in the literature. Second, they provide useful target values for those striving to create synthetic vitreous replacements.[23-25] Third, the steady-state network properties are quantitative and reproducible, suitable for quantifying the effects of pharmacological vitrectomy agents, examining natural and pathologic vitreous liquefaction, and also understanding the molecular architectures that produce the structure of the healthy vitreous. Equipped with an understanding of the primary structure of the vitreous and the tools to quantify changes in its mechanical properties, we are prepared to take a rational-design approach to vitreous engineering.

BIBLIOGRAPHY

1.   Bishop PN. Structural macromolecules and supramolecular organisation of the vitreous gel. *Progress in Retinal and Eye Research.* May 2000;19(3):323-344.

2.   Sebag J. *The Vitreous - Structure, Function, and Pathobiology.* New York: Springer-Verlag Inc.; 1989.

3.   Bos KJ, Holmes DF, Meadows RS, Kadler KE, McLeod D, Bishop PN. Collagen fibril organisation in mammalian vitreous by freeze etch/rotary shadowing electron microscopy. *Micron.* Apr 2001;32(3):301-306.

4.   Tokita M, Fujiya Y, Hikichi K. Dynamic viscoelasticity of bovine vitreous body. *Biorheology.* 1984;21(6):751-756.

5.   Pfeiffer HH. Zur analyse der fliess-elastizitaet durch spinnversuche am corpus vitreus. *Biorheology.* 1963;1:111-117.

6.   Bettelheim FA, Wang TJY. Dynamic Viscoelastic Properties of Bovine Vitreous. *Experimental Eye Research.* 1976;23(4):435-441.

7.   Lee B, Litt M, Buchsbaum G. Rheology of the vitreous body. Part I: Viscoelasticity of human vitreous. *Biorheology.* Sep-Dec 1992;29(5-6):521-533.

8.   Lee B, Litt M, Buchsbaum G. Rheology of the vitreous body: part 3. Concentration of electrolytes, collagen and hyaluronic acid. *Biorheology.* Jul-Aug 1994;31(4):339-351.

9.   Lee B, Litt M, Buchsbaum G. Rheology of the vitreous body: Part 2. Viscoelasticity of bovine and porcine vitreous. *Biorheology.* Jul-Aug 1994;31(4):327-338.

10.   Zimmerman RL. In Vivo Measurements of the Viscoelasticity of the Human Vitreous-Humor. *Biophysical Journal.* 1980;29(3):539-544.

11.   Walton KA, Meyer CH, Harkrider CJ, Cox TA, Toth CA. Age-related changes in vitreous mobility as measured by video B scan ultrasound. *Experimental Eye Research.* Feb 2002;74(2):173-180.

12.   Sebag J, Balazs E. Morphology and ultrastructure of human vitreous fibers. *Investigative Ophthalmology and Visual Science.* 1989;30:1867-1871.

13.   Nickerson CS, Kornfield JA. A "cleat" geometry for suppressing wall slip. *Journal of Rheology.* 2005;49(4):865-874.

14.   Weber H, Landwehr G, Kilp H, Neubauer H. The Mechanical-Properties of the Vitreous of Pig and Human Donor Eyes. *Ophthalmic Research.* 1982;14(5):335-343.

15.   Fatt I, Weissman BA. *Physiology of the Eye.* Second ed. Boston: Butterworth-Heinemann; 1992.

16.   Ferry JD. *Viscoelastic Properties of Polymers.* 3rd ed. New York: John Wiley & Sons; 1980.

17.   Flory PJ. *Principles of Polymer Chemistry.* Ithaca, NY: Cornell University Press; 1953.

18.   Rubinstein M, Colby RH. *Polymer Physics.* New York: Oxford University Press; 2003.

19.   Scott JE. Structure and function in extracellular matrices depend on interactions between anionic glycosaminoglycans. *Pathologie Biologie.* May 2001;49(4):284-289.

20.   Mendichi R, Soltes L, Schieroni AG. Evaluation of radius of gyration and intrinsic viscosity molar mass dependence and stiffness of hyaluronan. *Biomacromolecules.* Nov-Dec 2003;4(6):1805-1810.

21. Vogel S. *Comparative biomechanics: life's physical world.* Princeton, NJ: Princeton University Press; 2003.

22. Hasler EM, Herzog W, Wu JZ, Muller W, Wyss U. Articular cartilage biomechanics: Theoretical models, material properties, and biosynthetic response. *Critical Reviews In Biomedical Engineering.* 1999;27(6):415-488.

23. Dalton PD, Chirila TV, Hong Y, Jefferson A. Oscillatory shear experiments as criteria for potential vitreous substitutes. *Polymer Gels And Networks.* 1995;3(4):429-444.

24. Chirila TV, Hong Y, Dalton PD, Constable IJ, Refojo MF. The use of hydrophilic polymers as artificial vitreous. *Progress In Polymer Science.* 1998;23(3):475-508.

25. Soman N, Banerjee R. Artificial vitreous replacements. *Bio-Medical Materials and Engineering.* 2003;13(1):59-74.